Dissecting Packet Loss in Mobile Broadband Networks from the Edge

Džiugas Baltrūnas, Ahmed Elmokashfi, Amund Kvalbein
Simula Research Laboratory
Oslo, Norway

***Abstract*—This paper demonstrates that end-to-end active measurements can give invaluable insights into the nature and characteristics of packet loss in cellular networks. We conduct a large-scale measurement study of packet loss in four UMTS networks. The study is based on active measurements from hundreds of measurement nodes over a period of one year. We find that a significant fraction of loss occurs during pathological and normal Radio Resource Control (RRC) state transitions. The remaining loss exhibits pronounced diurnal patterns and shows a relatively strong correlation between geographically diverse measurement nodes. Our results indicate that the causes of a significant part of the remaining loss lie beyond the radio access network.**

I. Introduction

An increasing number of people and services rely on cellular mobile broadband (MBB) as their only network connection. This trend has transformed MBB networks into a critical infrastructure. The performance and stability of these networks tightly influence the daily routines of individuals and businesses. Performance degradations and outages can impact millions of users and disrupt vital services. Hence, measuring and dissecting the performance of MBB networks is of paramount importance to customers, operators, and regulators.

MBB performance and stability are not captured by a single metric but rather by several metrics that assess and quantify performance at different levels. This intricacy stems mainly from the stateful nature of mobile cellular networks. Before engaging in data exchange, the User Equipment (UE) needs first to attach itself to the network and establish a data exchange context with the relevant boxes in the cellular network. The completion of this step is the most basic level of performance that a user expects the network to offer. Being attached, however, does not guarantee a stable and reliable end-to-end data delivery. Hence, the ability to deliver data packets as reliably as possible is arguably the second most important aspect of performance in cellular MBB networks. Packet loss degrades the user experience and influences the performance of transport protocols and consequently the applications running on top of them. Quantifying the extent of packet loss in MBB networks and understanding its root causes are important steps towards understanding and improving MBB performance.

In this paper we study packet loss in four operational MBB networks in Norway. More specifically, we extend our previous work [3] by investigating whether we can quantify and explain loss using end-to-end measurements. We focus on end-to-end measurements to better understand how packet loss will affect the user experience. To this end, we use the Nornet Edge (NNE) infrastructure [10], which consists of hundreds of nodes for measuring MBB networks in Norway. Each node is connected to up to four MBB UMTS operators. These nodes are stationary and hosted in places like schools and government offices. They are distributed to be representative of (indoor and stationary) users in urban/suburban areas. We use these nodes to measure MBB packet loss. Further, we leverage connections' metadata to group connections from the same operator in order to gain insights into the root causes of packet loss. Specifically, we group connections by their serving cell and serving Radio Network Controller (RNC), and identify loss that affects several connections in one group at the same time. Our results give several invaluable insights into the nature and causes of loss in MBB networks. In summary, this paper makes the following contributions:

1) We present *the first large-scale study of packet loss in MBB networks*. The measurements are performed on the NNE infrastructure [10]. NNE is the largest infrastructure of its kind, with dedicated measurement nodes distributed over 100 Norwegian municipalities. The data used in this paper is captured from 341 nodes and four different operators over a period of one year. We observe clear differences in loss characteristics between operators. We further find that these differences can be attributed to how operators configure radio channel management.
2) We demonstrate that end-to-end active measurements augmented with a rich set of the connections' metadata can indeed *give invaluable insights into performance characteristics* of MBB networks.
3) By studying packet loss in light of connections' metadata, we manage to identify different sources of loss and compare the relation between loss and different aggregation levels inside the cellular networks. Our results inspired one of the operators we measured to revisit the configuration of its radio access network, which has lead to a dramatic decrease in packet loss.

II. Background and measurement infrastructure

This section gives an overview of the architecture of MBB UMTS networks and presents the infrastructure that was used to conduct our measurements.

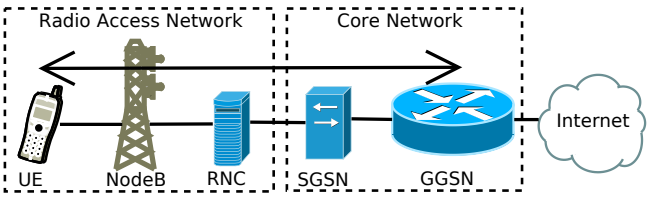

Fig. 1. Simplified architecture of an UMTS MBB network.

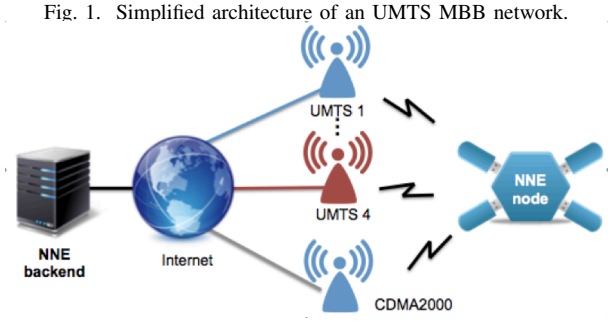

Fig. 2. NNE overview.

A. UMTS basics

Fig. 1 illustrates the various components that take part in the data forwarding in a typical MBB UMTS network divided into the Radio Access Network (RAN) and the Core Network (CN). A radio channel is created between a UE, which can be a modem or a smartphone, and the closest NodeB. NodeBs in the same geographical area are typically managed by the same RNC. Data packets are sent from the UE to its serving NodeB, which forwards them to the serving RNC, where they are in turn forwarded to the packet-switching CN. In the CN, packets travel through the Serving GPRS Support Node (SGSN) and Gateway GPRS Support Node (GGSN) before reaching the Internet. Note that the GGSN is the first IP hop on the path from the UE to any other host on the Internet. Before any data can be transmitted, the UE must attach itself to the network and establish a Packet Data Protocol (PDP) context towards the GGSN. The PDP context is a data structure that contains the IP address and other information about the user session. This state is a prerequisite for any communication between the UE and the Internet. Once a PDP context is established, the RNC allocates a shared or dedicated radio channel for the UE depending on the traffic pattern.

B. The Nornet Edge measurement platform and the data set

NNE (Fig. 2) is a dedicated infrastructure [10] for measurements and experimentation. It consists of several hundreds of measurement nodes geographically distributed all over Norway, and a well-provisioned server-side infrastructure, which is connected directly to the Norwegian research network UNINETT. Measurement nodes are placed indoors in both urban and suburban regions of Norway to reflect the population density of the country. Each measurement node is connected with up to four WCDMA and one CDMA network that provide MBB services in Norway. In this paper we consider WCDMA networks only, since the CDMA modems used by the platform provide a very limited set of connection state and location attributes.

Two of the four WCDMA networks to which NNE nodes are connected, *A* and *B*, have their own physical RANs *A* and *B*, while the other two, *C* and *D*, share the same RAN *S*. Subscribers of networks *C* and *D* use the shared RAN *S* where radio coverage is available. When outside their home network, connections of networks *C* and *D* camp on the RAN of networks *B* and *A* respectively. We did not have sufficient measurement points to characterize the shared RAN *S*, therefore we exclude it from parts of our analysis.

An NNE node is a custom-made single-board computer running a standard Linux distribution. 3G USB modems capable of HSPA+ (”3.75G”) are configured to prefer 3G networks when available, and fall back to 2G otherwise. In addition to the data service, the modems expose various metadata attributes, such as connection mode (e.g. 2G, 3G), signal strength, LAC, cell id and others. MBB connection management is governed by a dedicated connection management daemon running on all nodes. The daemon creates a network connection on all attached WCDMA modems and retries if it breaks. If the connection is successfully established, a PPP tunnel is created between the UE and the modem, which in turn establishes a PDP context with the GGSN.

The NNE backend contains the server-side of the measurements and handles configuration management, monitoring, data storage and post-processing, and other functions. NNE nodes run different experiments which are performed against measurement servers that are part of the NNE backend. Measurement results and metadata are transferred from the nodes to a backend database periodically. During the measurement period, the number of simultaneously active measurement nodes varied between 108 and 253.

III. Packet Loss Statistics

This section looks at the overall statistics and characteristics of measured packet loss. Using continuous end-to-end probing and rich connection metadata, we report on per-connection packet loss. We further investigate the interplay between radio channel types and radio resource control on the one hand and packet loss on the other.

A. Measurement Description

To measure packet loss, we send a 20 byte UDP packet to an echo server every second, and record the reply packet from the server. Every request-response pair is logged and later imported into a database. We include a timestamp and an incremental sequence number in the packet payload for duplicate detection and round-trip time calculations. While the round-trip time is normally on the order of tens of milliseconds, we sometimes observe delays of several seconds. Such high values can be caused by repeated link-layer retransmissions and excessive buffering [8]. We consider a packet to be lost if we do not receive a reply within 60 seconds.

This measurement script runs at all times on all measurement nodes. It starts automatically on all network interfaces as they become active, and keeps running as long as the interface is up. When the connection is not available, the

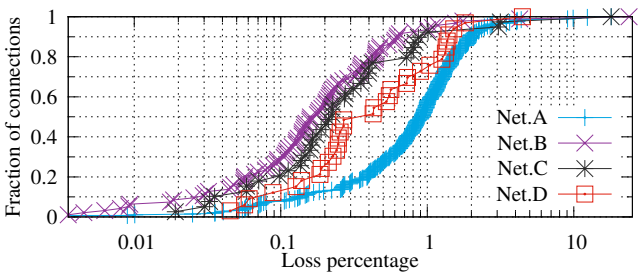

Fig. 3. Loss rate for each MBB operator. We see clear differences between operators.

measurement script stops sending packets and waits until the connection is active again. In total, we collected more than 13 billion data points from 341 distinct nodes from June 2013 to July 2014. The measurement duration of each connection varies depending on how long the node was available and had working connections. In the following analysis, we only include connections that contribute at least one week of measurements. To avoid any artifacts that could be caused by poor coverage, we only include connections that have an average signal strength greater than -102 dBm. Further, as some of our connections experience mode switches from 3G to 2G and vice versa, leading to excessive packet loss, we only include data from periods when connections were predominantly on 3G. Additionally, we filter out maintenance window periods and cases in which we had problems with our infrastructure. Lastly, in our analysis we consider only the data when the measurement script was able to send 300 packets via a single MBB connection during a five-minute interval. We do this to avoid introducing packet loss, which might happen right after the PDP context is established or before abnormal termination.

B. Loss rate

Fig. 3 shows the CDF of overall loss rate per connection for all operators. For each connection, the loss rate is defined as (the number of lost packets)/(the number of sent packets). Loss is relatively small in all networks; at least 50% of connections experience less than 1% packet loss across operators. We also see clear differences between operators. 72% of Net.A connections suffer more than 0.5% loss, whereas this ratio is between 15% and 43% for the other networks. As for the fraction of connections with excessive packet loss (e.g. a few percents), we do not measure clear differences between networks.

Loss patterns in Net.B and Net.C show clear similarities, and half of Net.C and Net.D connections show comparable loss. Furthermore, the worst 20% of Net.A and Net.D connections exhibit similar loss. These observations hint at different loss components that lie both in the RAN and beyond it. Recall that Net.C and Net.D own the same RAN which covers only some parts of the country. Outside areas covered by their RAN, Net.C and Net.D use RAN B and RAN A respectively. All networks, however, operate separate CNs.

C. The role of radio resource control

Once the UE successfully attaches itself to the MBB network, it proceeds by asking the RNC to allocate radio resources. Following this, the RNC assigns the UE to either a shared or dedicated channel depending on the user's traffic pattern. In 3G UMTS networks, a UE's RRC connection can be in one of four RRC states depending on the allocated channel or its lack thereof. Based on the bit rate, the UE can be assigned a CELL_FACH (shared channel, low bit rate, low power usage) or CELL_DCH state (dedicated channel, high bit rate, high power usage). If the UE is not sending any data, its RRC state is set to CELL_PCH or IDLE. No radio resources are allocated to UEs in these states and thus they cannot send data. The transitions between these states are regulated by bit-rate and inactivity timers [6].

Radio states differ in available resources and consequently performance, hence it is important to control for their effect when analyzing packet loss. Our connections are either on CELL_FACH or CELL_DCH, since they continuously send data. Connections that only send 20-byte UDP pings remain on CELL_FACH. Note that the connections we use for remotely managing measurement nodes and for transferring measurement logs are typically on CELL_DCH. To understand the effects of RRC state on packet loss, we divide our measurement period into consecutive five-minute bins. We then classify each connection bin into one of four categories based on the recorded RRC states within it:

1) **DCH.** A connection bin is classified as DCH if the connection was on CELL_DCH throughout the bin.
2) **FACH.** A connection bin is classified as FACH if the connection was on CELL_FACH throughout the bin.
3) **Mixed-UP.** These are connection bins in which connections experience either state promotion from CELL_FACH to CELL_DCH or a demotion in the opposite direction.
4) **Mixed-Downgraded.** These are connection bins in which connections experience a state demotion to CELL_PCH or IDLE. Note that this should not happen since our connections are always sending data.

After classifying all connection bins, we calculate the fraction of time spent and loss induced on different RRC categories for each operator. Specifically, we sum all connection bins and lost packets in them from the same operator, which gives the total number of measurement bins we collected and the total number of lost packets for this operator. We then calculate the number of these bins that are in different RRC categories. Table I presents the results of these calculations. The most important observation is that all operators spend some time in the Mixed-Downgraded state, which reflects unexpected pathological behavior. It also shows that most loss happens while on Mixed-Downgraded for all networks except Net.B, where loss induced in DCH and Mixed-Downgraded is similar. According to the 3GPP standards, as long connections are actively engaged in data exchange, they should never be demoted to IDLE or CELL_PCH. We note that these

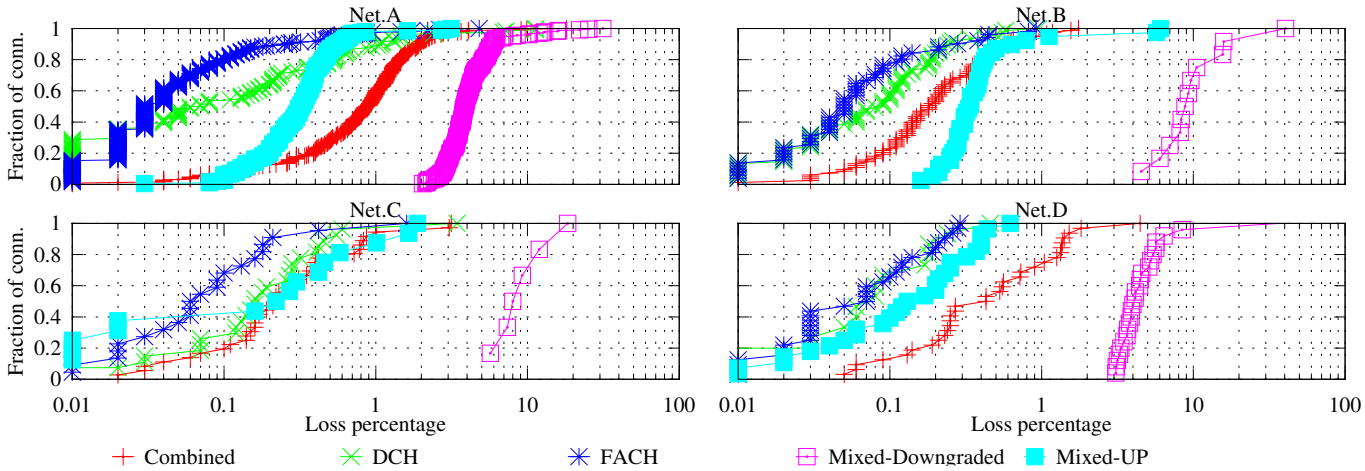

Fig. 4. Loss rate experienced during different RRC bins. We record very high loss rate during periods with state transitions.

transitions happen to connections on DCH as well as to connections on FACH. The presence of such demotions indicates that they are not strictly inactivity based. This pathological behavior is most evident in Net.A and Net.D. Recall that Net.D connections use RAN A in locations not covered by their RAN. This indicates that the observed pathological behavior is RAN-related, which is consistent with the fact that RRC states are managed by RNCs.

Overall, connections that use RAN A undergo markedly more state transitions, including both pathological and standard promotions and demotions compared to connections that use other RANs. Additionally, the percentage of time spent on FACH and DCH also varies widely across operators. This is mainly an artifact of the way NNE connections are used for tasks other than sending the 20-byte pings. For instance, in nodes with UMTS connectivity only, logs and measurement data are transferred over Net.B and Net.C connections, which explains why these two operators spend much more time on DCH.

TABLE I
TIME SPENT (TS) AND LOSS INDUCED (LI) BY EACH NETWORK ON DIFFERENT RRC CATEGORIES.

Net.	TS LI	FACH	DCH	Mixed-UP	Mixed-Downgraded
Net.A	TS	56.3%	4.4%	21%	18.3%
	LI	4.7%	1.9%	9.6%	83.7%
Net.B	TS	26.8%	59.2%	13.3%	0.7%
	LI	9.4%	35.9%	19.2%	35.5%
Net.C	TS	35.2%	60.4%	2.3%	2.2%
	LI	12.1%	32%	2.3%	53.6%
Net.D	TS	64.2%	5.2%	19.2%	11.5%
	LI	6.8%	0.8%	6.3%	86%

Knowing the RRC categories in which our connections spend the most time and which carry the most loss, we now move to measuring the loss rate of individual connections for each category. For each connection, the loss rate while in category C_i is defined as (the number of lost packets while on C_i)/(the number of sent packets while on C_i). The four panels in Fig. 4 show the loss rate in each category for all four operators. Across the board, Mixed-Downgraded stands

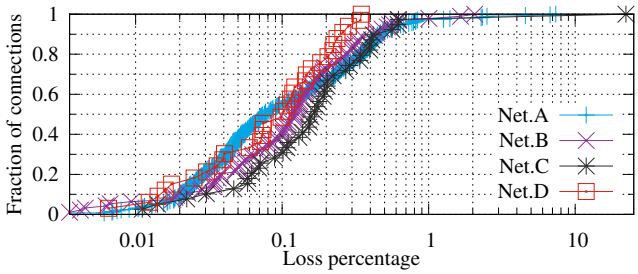

Fig. 5. Loss rate for each MBB operator considering only non-pathological states.

out as the lossiest category, in accordance with the induced loss numbers in Table I. This is expected since Mixed-downgraded corresponds to cases in which connections are demoted to IDLE or CELL_PCH. In these states connections lose their data connection to the network and hence are not able to exchange data. Loss in periods with regular state transitions (i.e. Mixed-UP) is the second worst. In such five-minute bins, a connection spends a fraction of the time in FACH, another fraction in DCH, and a short period transiting between them. We expect loss during the combination of FACH and DCH states to be comparable to the loss in FACH and DCH categories separately. Hence, we believe that the difference in loss between Mixed-UP periods and FACH (DCH) periods is mainly due to transitions between states. Investigating this further with one of the four operators studied confirmed that. Loss can happen during transitions because the UTRAN Radio Link Control Protocol (RLC), a protocol responsible for interfacing between upper layers and the MAC layer [6], has different Service Data Unit (SDU) sizes for FACH and DCH. Interestingly, differences between FACH and DCH are mostly minor. Thus RLC SDUs in transit must be buffered when undergoing state transitions [14] and retransmitted once they are complete. In fact, the mentioned operator did not have the retransmission enabled during the RLC re-establishment beforehand, which affected many applications using unreliable transport protocols, such as UDP.

The breakdown of loss along RRC states gives more insights into the measured differences between operators (See Fig. 3).

Net.A exhibits more loss because it spent ≈ 40% of the time in Mixed-Downgraded and Mixed-UP. Net.D exhibits less loss, although it spent ≈ 30% of the time in these two states. Looking closer at Net.D, we find that the excessive loss in Mixed-Downgraded is offset by negligible loss in the other three categories. Fig. 5 illustrates the CDF of the overall loss when considering only loss that happens in FACH, DCH, and Mixed-UP bins. Overall, loss decreases significantly, at most 9% of connections experience loss more than 0.5%. Further, differences between operators become less pronounced. Hence, avoiding these pathological transitions can greatly reduce loss. These results inspired Net.A to revisit its configuration: enable inactivity based timer for the FACH to PCH transition (previously the transition was happening when maintaining a low bit rate); enable packet retransmission during RLC re-establishment; and few other changes on their RNCs. This has resulted in a major reduction in pathological transitions and overall loss rate (see Sec. VI).

Summary of findings. Our results demonstrate clear differences in packet loss between operators, and show that most loss is caused by RRC state transitions, both pathological and standard. The former transitions force active connections into idle and paging modes, deallocating the radio resources they need for sending data. We expect differences between operators to diminish if pathological transitions are avoided.

IV. Correlations in loss

In order to reduce packet loss, we first need to pinpoint its potential causes. To this end, we correlate loss measured for pairs of connections from the same operator. We perform these correlations at the operator level, RNC-level, and cell-level to determine whether observed loss is independent or caused by events that impact multiple connections simultaneously (e.g. network congestion and outages).

To correlate a pair of connections, we divide each connection UDP-ping time series into five-minute bins, and calculate the loss ratio in each bin. We use these time series to determine the likelihood that this pair of connections experiences loss equal to or greater than X% in the same five-minute bin. Let $P(A)$ denote the (empirical) probability that a connection A has a loss rate equal to or greater than X% in a given five-minute bin, and $P(B)$ denote the same for a connection B. We calculate the conditional probability $P(A|B)$ of A having loss given that B has loss and compare it to the unconditional probability $P(A)$. If the conditional probability ratio $R = P(A|B)/P(A)$ is close to 1, it means that connections A and B experience loss largely independently, while a high R means that they tend to experience loss together. Note that by Baye's law, $P(A|B)/P(A) = P(B|A)/P(B)$. We have experimented with setting X to 1%, 3%, and 5% packet loss which mostly gave qualitatively similar results. In the rest of this section, we stick to the 3% threshold (i.e. the loss of at least nine packets in a five minute-bin) to avoid any spurious correlations that $X = 1\%$ may cause as well as to avoid focusing only on rare loss events which limit us to 5% or more loss. The loss in bins with 3% or more packet loss is between 75% and 91% of the overall loss depending on the operator.

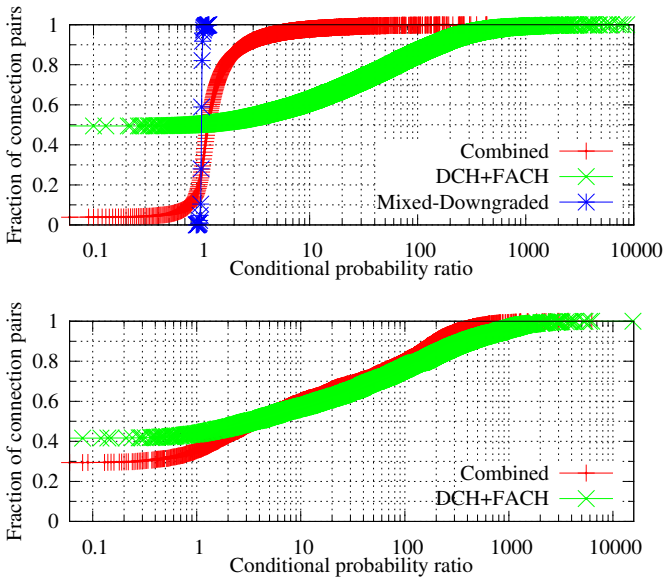

Fig. 6. Correlations for loss ≥ 3% in different RRC categories for RAN A and RAN B. Loss in DCH and FACH exhibits relatively strong correlations.

A. Operator-wide correlations

Thus far, our findings show that pathological state transitions are responsible for a significant fraction of the measured packet loss. It is unclear, however, whether this loss is correlated (e.g. these transitions happen because of a sub-optimal RNC configuration that affects several connections simultaneously). To verify this, we calculate the conditional probability ratio R for all pairs of connections from the same operator considering all measured five-minute bins. We also calculate the same ratio correlating only bins of certain RRC category. In other words, for each connection, we construct two additional time series. The first time series include all five-minute bins in which the connection was on Mixed-Downgraded, the second involves bins of the three non-pathological types DCH, FACH, and Mixed-UP, which we refer to as DCH+FACH.

The plots in Fig. 6 present the CDF of R for different RRC states for RAN A and RAN B. In the remainder of this paper, we leave RAN S aside because of its small sample size. When correlating bins regardless of their RRC state (denoted as "Combined" in the figure), RAN A demonstrates little correlation with 90% of the connection pairs having $R \leq 2$. RAN B, however, appears more correlated, with only 40% of pairs having $R \leq 2$. Both RANs are, however, characterized by a lack of correlation for loss related to pathological state transitions. For RAN A, loss in Mixed-downgraded is independent with $R \approx 1$. For RAN B, there is not a single correlated pathological bin, which explains why Mixed-Downgraded is missing in the lower panel. Furthermore, DCH+FACH demonstrates strong correlations for both operators, with about 40% of connection pairs having $R \geq 10$. We note that for connection pairs in the FACH+DCH category with $R \leq 2$, the median common measurement period (i.e. the time in which both

connections were present) is 60 days and 93 days for RAN A and RAN B respectively. These periods are long enough to observe rare network events and to avoid spurious correlations. Furthermore, R equals zero for about 50% (40%) of pairs in RAN A (RAN B) meaning that there is not a single common lossy bin. Investigating these pairs shows that they have more than three times less common measurement period compared to pairs with $R \leq 2$. Hence, this lack of correlation can be attributed to the interplay between the relatively short common measurement periods and the measured rarity of excessive loss in MBB in general. In other words, we need longer common periods, as we have for pairs with $R \leq 2$ to be able to identify correlated loss. Based on these observations, we note the following points. Loss during pathological RRC transitions impacts connections independently. Further, correlating loss bins that are characterized by different RRC states may lead to spurious conclusions. For example, loss in RAN A appears uncorrelated if we do not split it according to the RRC state.

The strong correlation in loss during DCH+FACH suggests that the causes of this loss do not affect connections individually. Possibly, these causes are related to components in the MBB network that serve multiple connections simultaneously (e.g. NodeB, RNC, or GGSN). The remainder of this section investigates the role of such components by evaluating correlations in DCH+FACH loss at the RNC and cell levels.

B. RNC-level correlations

To be able to perform RNC-level correlations, we first need to map connections to RNCs. NNE collects a rich set of metadata about connections, including the Location Area Code (LAC) and the UTRAN CELL ID (LCID). The former indicates a group of towers that are served by the same RNC. However, there is no one-to-one mapping between LACs and RNCs. The latter is a 6-byte hexadecimal value, the first 2-bytes represent the serving RNC-ID, while the other 4-bytes represent the Cell-ID. We use this to determine the RNCs that serve RAN B connections. Unfortunately, RAN A sets the RNC-ID bits to the first digits of LAC, but not the real RNC identifier. Hence, we resort to using an RNC coverage map provided by Net.A that indicates all RNCs and their geographic scope. RAN A comprises 12 RNCs, while RAN B comprises 14. The number of connections served by each RNC depends on the NNE nodes' deployment. The percentage of connections per RNC varies from 2.4% to 25.5% for RAN A and from 0.8% to 19.7% for RAN B. We have more connections associated with RNCs that serve the three largest cities in Norway.

We calculate the conditional probability ratio for all connection pairs that are served by the same RNC, which we refer to as the intra-RNC correlation. We only consider pairs that shared the same RNC for at least one week. In addition, we correlate pairs of connections that are not served simultaneously by the same RNC, which we refer to as inter-RNC correlation. Note that we are only correlating loss that happens in DCH+FACH. Fig. 7 shows the CDF of inter-RNC and intra-RNC correlations for RAN A and RAN B. For both

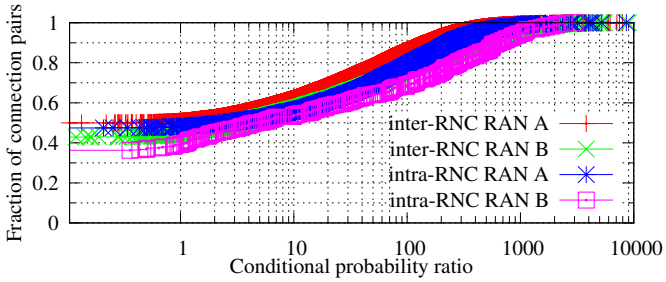

Fig. 7. Correlation in loss for connections served by the same RNC vs connections served by different RNCs.

RANs, differences between intra-RNC correlations and inter-RNC correlations are very negligible. Note that correlations for both groups remain high, suggesting that the causes of these correlations lie beyond the RAN. Next, we investigate how many correlations at the RNC level can be attributed to correlations at the cell level.

C. Cell-level correlations

In order to study cell-level correlations, we need to have an adequate number of connection pairs that are served by the same cells simultaneously. Unfortunately, the NNE measurement infrastructure was not deployed such that it maximizes the number of measurement nodes covered by the same cell towers. This makes the task of finding connections that share serving cells difficult. We scan our data set to identify connections that attach to the same cells simultaneously by looking at two types of nodes. First, nodes that are in the same cell tower ranges, thanks to NNE dense deployment in the three largest cities in Norway. Second, nodes that have two connections served by the same RAN (e.g. a Net.A connection and a Net.D connection that camps on RAN A). These two connections are essentially served by the same cells and the same RNCs. We identify 34 and 31 cells belonging to RAN A and RAN B respectively that serve multiple connections simultaneously. Note that the overall number of distinct cells in our data set is 1988 for RAN A and 458 for RAN B.

We calculate the conditional probability ratios for all connection pairs that are served by the same cells, which we refer to as the intra-cell correlation. We only consider pairs that shared the same cell for at least one week. In addition, we correlate pairs of connections that are not served simultaneously by the same cells, which we refer to as the inter-cell correlation. Note that we are only correlating loss that happens in DCH+FACH. Fig. 8 shows the CDF of inter-cell and intra-cell correlations for RAN A and RAN B. For both RANs, intra-cell correlations are mostly higher than inter-cell correlations. Inter-cell correlation is reasonably high (R $\geq$ 10) for a sizable fraction of pairs, but it is less than compared to the above presented operator-wise and inter-RAN correlations. We get $R = 0$ for about 80% of inter-cell pairs in RAN A and 65% of inter-cell pairs in RAN B. These numbers are higher than their network-wide and RNC counterparts. These discrepancies stem from the fact that our inter-cell and intra-cell pairs have very short common periods compared to

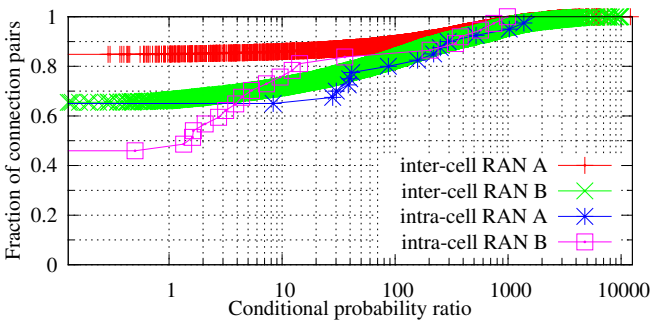

Fig. 8. Correlation in loss for connections served by the same cell vs connections served by different cells.

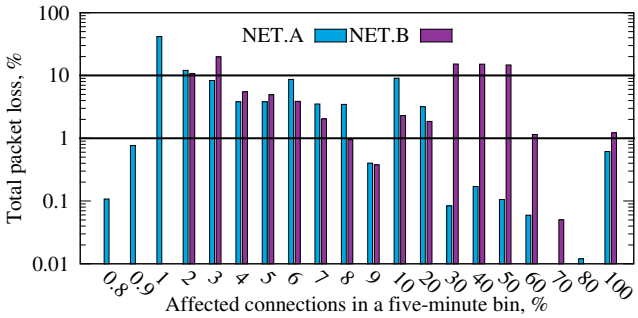

Fig. 9. Loss rate quantification for MBB networks A and B.

network-wide pairs or RNC pairs. For instance, the median common measurement period for intra-cell pairs is 10 days for RAN A and 15 days for RAN B. A typical connection in our data set alternates between 3 or 4 cells, so a pair of connections in the range of the same group of cells may end up connecting to different cells within the group reducing the common measurement period. These periods are too short when measuring correlations in loss given the demonstrated rarity of excessive loss in MBB. To confirm this, we re-calculate the inter-cell and intra-cell correlations considering five-minute bins with loss $\geq 1\%$ (i.e. greater likelihood of loss). We find that the differences between inter-cell and intra-cell correlations diminish, giving results similar to the RNC-level correlations.

Summary of findings. The results of this section show that loss experienced during the pathological Mixed-downgraded transition is highly uncorrelated. Hence, these transitions reflect a behavior that affects individual connections rather than several connections simultaneously. The loss experienced during DCH+FACH, however, exhibits a strong correlation. We measure a negligible difference in the likelihood of simultaneous loss between connection pairs served by the same RNC and those served by different RNCs. This suggests that the measured RNCs are not congested. The same is true at the cell-level if we control for the length of the common measurement period. Finally, we note that the presence of strong correlations between arbitrary connection pairs hints at causes that lie beyond the RAN.

V. Possible causes

Our results indicate that there is a non-trivial fraction of correlated loss. Further, the causes of these correlations seem to lie beyond the RAN. This section makes one step closer to understanding potential causes of loss.

A. Impact of the loss episodes

The pairwise correlations presented in the previous section only show whether a connection pair is likely to experience loss at the same time. It does not show how many connections in total experience loss simultaneously. The number and location of connections that suffer loss at the same time give an idea about where the root causes lie. For instance, if the number of impacted connections is high and these connections are served by different RNCs, then the root cause lies beyond the RAN. Hence, in order to identify the root causes of most loss, we need to to quantify how much of the overall loss is related to loss episodes that impact a few connections as opposed to those impact a significant fraction of connections.

To measure that, for each connection we identify all five-minute bins with loss equal to or greater than 3%. Next, we merge bins from all connections, giving us a list of all five-minute bins where at least a single connection experiences 3% or more loss. Every bin is, therefore, characterized by two numbers: the number of affected connections, and the number of lost packets on all affected connections. We use these two numbers to quantify how many loss episodes with a given number of affected connections contribute to all packets in bins with loss $\geq 3\%$. We limit ourselves to bins with loss $\geq 3\%$ to avoid spurious correlations. Further, the majority of loss happens in these bins (i.e. between 71% and 91% of the overall loss depending on the RAN).

Fig. 9 shows histograms of the percentage of packets lost, binned by the percentage of connections impacted, for Net.A and Net.B. The two horizontal lines mark the 1% and 10% loss levels. We record clear differences between the two operators. Net.B's histogram exhibits several pronounced modes for the impact range between 30% and 60% of connections. One third of the loss happens in bins where $1/3$ or more connections are affected. Net.A histogram also exhibits clear modes but they correspond to much smaller impact ranges. About half of the loss happens in bins where 2% or fewer connections are affected and $\approx$ 84% of all loss happens in bins where 10% or fewer connections are affected. Furthermore, for both networks loss episodes that impact all connections simultaneously account for 1% of overall packet loss.

Our findings indicate that Net.B is more prone to loss episodes that affect a large fraction of connections simultaneously. This fraction (i.e. over one third) is evidently higher than the percentage of connections served by the most populous RNC in RAN B (19.7%). Hence, the root causes of this highly correlated loss lie in the CN or in the interconnection between Net.B and the Internet. In contrast, Net.A is less prone to episodes that impact a large fraction of connections simultaneously, suggesting that Net.A's core is better provisioned than Net.B's. Note that, despite the rarity of widely correlated loss in Net.A, a sizable fraction of loss (16%) happens in bins

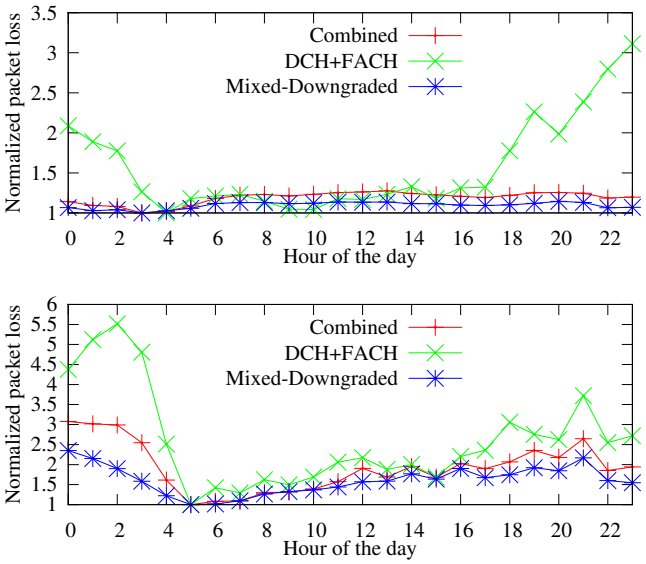

Fig. 10. Diurnal patterns of loss in RAN A and RAN B. DCH+FACH loss climbs rapidly during peak hours.

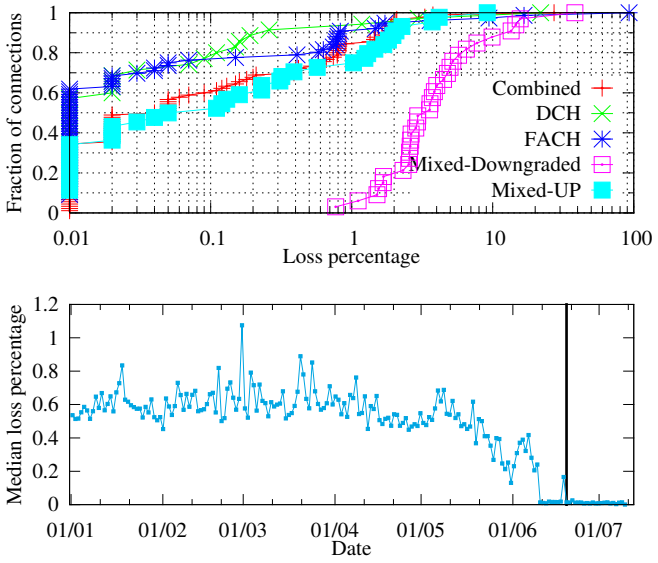

Fig. 11. Loss rate by RRC state (top) and median loss rate (bottom) for Net.A after the RNC reconfiguration.

where 10% or more geographically-diverse connections are affected.

B. Diurnal patterns in loss

Network congestion is a possible cause for loss in the CN. To investigate this, we calculate average hourly loss per RRC category for each operator. Fig. 10 shows variations in the average hourly loss per RRC category normalized by the smallest value in the respective category.

Loss in DCH+FACH demonstrates distinct diurnal patterns for both operators. Average hourly loss climbs after 15:00 GMT, which is about the time that people leave work. Before midnight loss at least triples. The average hourly loss for Net.A decreases slowly after that until it reaches a minimum at around 4 AM. Net.B, however, exhibits a strong peak at 2 AM. We suspect that this peak is related to periodic maintenance activity in Net.B. Note that Mixed-Downgraded does not show a strong diurnal component. Interestingly, the identified diurnal patterns do not coincide with expected peak hours for mobile users (i.e. during business hours). Instead, they match residential broadband peak hours suggesting two plausible causes. First, loss increases as MBB traffic mixes with residential traffic; both studied MBB providers are also fixed broadband providers. Second, more users depend on MBB as their only connection to the Internet resulting in traffic peaks comparable to fixed broadband.

Summary of findings. This section shows that a significant fraction of loss is related to episodes that simultaneously impact a significant fraction of geographically-diverse connections. Further, loss in DCH+FACH is characterized by strong diurnal patterns. These findings suggest that congestion is a plausible cause for loss in DCH+FACH.

VI. Discussion

In the previous sections, we identified two potential causes of loss: pathological and lossy state transitions; and congestion. Our findings confirm the conventional wisdom that losing packets on the MBB radio interface is rare, especially for reasonably covered stationary connections, thanks to the retransmission-aggressive nature of MBB link-layer protocols. Hence, a lossy MBB network is indicative of a sub-optimally configured RAN or a congested CN. Congestion can be addressed by re-dimensioning and increasing the capacity of the RAN and CN. However, mitigating loss caused by pathological and regular state transitions requires optimizing the RAN configurations. RNCs must not demote users to IDLE as long as they are sending data; such state demotion must strictly be decided by inactivity timers. Also, in flight RLC SDUs need to be buffered during state transitions to account for the mismatch between the SDUs of different channels [2].

Our results inspired Net.A to revisit its RNC configuration to reflect the aforementioned fixes. The top panel in Fig. 11 shows the CDF of loss percentage after the application of configuration changes in Net.A. The overall loss dropped markedly, and loss in Mixed-UP is similar to loss in FACH and DCH. Further, differences between Mixed-UP, FACH, and DCH decreased. After the change, the percentage of time Net.A spent on Mixed-Downgraded bins dropped from 19% to only 0.98%. The lower panel shows the median daily loss percent in Net.A measured for all connections, from 01/01/2014 to 10/07/2014. The change took place on 19/06/2014 (marked by the vertical line), where we see a sudden drop in median loss. Following the configuration changes, median loss dropped from about 0.6% to almost zero. This indicates that slight changes to the way the RRC state machine is managed and to the way in-flight data packets are handled during RRC state promotions and demotions can reduce loss significantly. We believe that many operators world-wide would benefit from our observations and the suggested fixes.

VII. Related work

In the past few years, there have been a number of initiatives to measure MBB networks. Approaches can be classified into three categories: *crowd-sourced user initiated measurements* [1, 11, 19], *measurements collected using dedicated infrastructures* [9, 16], and *measurements based on network-side data* [5, 7, 17, 18]. While all three approaches have their strengths, we find it difficult to rely on user-initiated measurements for the continuous monitoring of MBB networks' stability. Furthermore, network-side logs are typically only available to operators. Our study runs end-to-end measurements from a dedicated infrastructure consisting of several hundreds of measurement nodes. This not only gives us full control over all components of the ecosystem, but also produces a dataset of better quality with fewer artifacts. To the best of our knowledge, there has been no comprehensive study of packet loss using end-to-end measurements in 3G networks. Perala et al. [12] showed that operators do not necessarily configure their RRC state machine in accordance with standard literature. The effects of RRC state transitions and the impact of state promotion delays on application performance has been studied by Qian et al. [13] and Rosen et al. [15]. Xu et al. [20] showed that downlink traffic can be buffered in the network, causing bursty packet arrivals. In this context, they additionally investigated a drop policy enforced by the network and discovered that the drop-tail policy is typically used to drop packets. Chen et al. [4] studied RNC-level performance with an aim to understand main driving factors. Using TCP-level packet retransmission rates they found that RTTs and loss rates were correlated, suggesting a connection between time dependent factors and the size of a flow. It has been noted that in some cases loss is caused by NodeBs during highly loaded periods. Huang et al. [7] conducted a large-scale study showing the impacts of protocols and applications on LTE network performance. Using the data collected from a proxy in the CN, they show that most transport-layer packet loss is related to physical layer retransmissions and can be reduced by buffering.

VIII. Conclusions

This work presents an exhaustive large scale end-to-end measurement of loss in cellular networks. Our results demonstrate that end-to-end measurements can give insights into the performance of cellular network internals. We find that most loss is a direct result of RRC state transitions, both regular and pathological. The remaining loss is mostly due to activity in the CN. Loss exhibits strong diurnal patterns and is related to performance degradation episodes that simultaneously impact a significant fraction of geographically-diverse connections. Our results motivated one of the operators measured to re-examine its network configuration to mitigate loss caused by state transitions. This clearly highlights the importance of independent end-to-end measurement infrastructures like NNE, which allows correlating measurements at different levels and spot potential problems in MBB networks. Going forward, we plan to look at loss experienced on the move, where we expect to see new effects related to handovers and continuous changes in connection types.

References

[1] Mobiperf. http://www.mobiperf.com, 2014.

[2] J. Alcaraz, F. Cerdan, and J. Garcia-Haro. Optimizing TCP and RLC interaction in the UMTS radio access network. In *IEEE Network*, 2006.

[3] D. Baltrūnas, A. Elmokashfi, and A. Kvalbein. Measuring the Reliability of Mobile Broadband Networks. In *Proc. of IMC*, 2014.

[4] Y. Chen, N. Duffield, P. Haffner, W. ling Hsu, G. Jacobson, Y. Jin, S. Sen, S. Venkataraman, and Z. li Zhang. Understanding the Complexity of 3G UMTS Network Performance. In *IFIP Networking Conference*, 2013.

[5] E. Halepovic, J. Pang, and O. Spatscheck. Can you GET me now?: Estimating the time-to-first-byte of HTTP transactions with passive measurements. In *Proc. of IMC*, 2012.

[6] H. Holma and A. Toskala. *WCDMA for UMTS: HSPA Evolution and LTE*. John Wiley & Sons Ltd., 4th edition, 2007. ISBN 9780470512531.

[7] J. Huang, F. Qian, Y. Guo, Y. Zhou, Q. Xu, Z. M. Mao, S. Sen, and O. Spatscheck. An In-depth Study of LTE: Effect of Network Protocol and Application Behavior on Performance. In *Proc. of SIGCOMM*, 2013.

[8] H. Jiang, Y. Wang, K. Lee, and I. Rhee. Tackling Bufferbloat in 3G/4G Networks. In *Proc. of IMC*, 2012.

[9] Z. Koradia, G. Mannava, A. Raman, G. Aggarwal, V. Ribeiro, A. Seth, S. Ardon, A. Mahanti, and S. Triukose. First Impressions on the State of Cellular Data Connectivity in India. In *Procs. of ACM DEV-4*, ACM DEV-4 '13, 2013.

[10] A. Kvalbein, D. Baltrūnas, J. Xiang, K. R. Evensen, A. Elmokashfi, and S. Ferlin-Oliveira. The Nornet Edge platform for mobile broadband measurements. *Elsevier Computer Networks special issue on Future Internet Testbeds*, 2014.

[11] A. Nikravesh, D. R. Choffnes, E. Katz-Bassett, Z. M. Mao, and M. Welsh. Mobile Network Performance from User Devices: A Longitudinal, Multidimensional Analysis. In *Procs. of PAM*, 2014.

[12] P. Perala, A. Barbuzzi, G. Boggia, and K. Pentikousis. Theory and Practice of RRC State Transitions in UMTS Networks. In *IEEE GLOBECOM Workshops*, 2009.

[13] F. Qian, Z. Wang, A. Gerber, Z. M. Mao, S. Sen, and O. Spatscheck. Characterizing Radio Resource Allocation for 3G Networks. In *Proc. of IMC*, 2010.

[14] F. Qian, Z. Wang, A. Gerber, Z. M. Mao, S. Sen, and O. Spatscheck. Profiling resource usage for mobile applications: A cross-layer approach. In *Procs. of MobiSys*, 2011.

[15] S. Rosen, H. Luo, Q. A. Chen, Z. M. Mao, J. Hui, A. Drake, and K. Lau. Discovering Fine-grained RRC State Dynamics and Performance Impacts in Cellular Networks. In *Proc. of Mobicom*, 2014.

[16] S. Sen, J. Yoon, J. Hare, J. Ormont, and S.Banerjee. Can they hear me now?: A case for a client-assisted approach to monitoring wide-area wireless networks. In *Proc. of IMC*, 2011.

[17] M. Z. Shafiq, L. Ji, A. X. Liu, and J. Wang. Characterizing and Modeling Internet Traffic Dynamics of Cellular Devices. In *Proc. of SIGMETRICS*, 2011.

[18] M. Z. Shafiq, L. Ji, A. X. Liu, J. Pang, S. Venkataraman, and J. Wang. A first look at cellular network performance during crowded events. In *Proc. of SIGMETRICS*, 2013.

[19] J. Sommers and P. Barford. Cell vs. WiFi: On the Performance of Metro Area Mobile Connections. In *Proc. of IMC*, 2012.

[20] Y. Xu, Z. Wang, W. Leong, and B. Leong. An End-to-End Measurement Study of Modern Cellular Data Networks. In *Proc. of PAM*, 2014.